Novel Surface Modifying Macromolecules (SMMs) Blended Polysulfone Gas Separation Membranes by Phase Inversion Technique

Houman Savoji,[1,2] Dipak Rana,[1] Takeshi Matsuura,[1] Mohammad Soltanieh,[2] Shahram Tabe[3]

[1]*Industrial Membrane Research Institute, Department of Chemical and Biological Engineering, University of Ottawa, 161 Louis Pasteur St., Ottawa, ON, Canada K1N 6N5*
[2]*Department of Chemical and Petroleum Engineering, Sharif University of Technology, Tehran, Iran*
[3]*Standards Development Branch, Ministry of the Environment, Toronto, Ontario M4V 1M2, Canada*

Received 8 December 2010; accepted 27 April 2011
DOI 10.1002/app.34809
Published online 24 August 2011 in Wiley Online Library (wileyonlinelibrary.com).

ABSTRACT: In this article an attempt was made to fabricate defect-free asymmetric polysulfone (PSf) membranes for the separation of oxygen and nitrogen. The approach is based on the enhanced delayed demixing by blending surface modifying macromolecules (SMMs) in the casting solution and by immersing the cast film in isopropanol for a certain period before it is immersed in water. Different SMMs, including hydrophobic and charged SMMs, were synthesized, characterized, and blended to the host PSf. It was found that the charged SMM could indeed contribute to the removal of defective pores from the skin layer and enhancement of oxygen/nitrogen selectivity. The experimental results were further interpreted based on the shift of the phase boundary line on the polymer/solvent/nonsolvent triangular diagram, which occurred when SMMs were blended to PSf, due to the change in the polymer/nonsolvent interaction. © 2011 Wiley Periodicals, Inc. J Appl Polym Sci 124: 2287–2299, 2012

Key words: surface modifying macromolecules; polysulfone; gas separation membranes; defect free asymmetric membranes; wet/wet phase inversion method

INTRODUCTION

Fabrication of asymmetric membranes with defect free skin layers has been the subject of numerous attempts since the first application of polymeric membranes in gas separation. Pinholes in the skin layer, even of small numbers, cause the feed gas leak, lowering the selectivity of the membrane.

To overcome this problem, Henis and Tripodi[1] proposed in 1981 sealing the defective pores of asymmetric membranes using silicone rubber. This innovative idea led to the commercialization of Prism membrane. According to their method, a relatively thick silicone rubber layer is coated over a thin skin layer. The silicone rubber penetrates into the pores and plugs them. Thus, by preventing the leakage of feed gas through defective pores the selectivity of the membrane approaches that of a defect-free one. Moreover, since the gas permeability of silicone rubber is orders of magnitude higher than those of the base membrane the permeation rate remains almost the same as the membrane with a skin layer without defects.

Despite commercial success, the Henis and Tripodi's method suffered from the need to fabricate the membranes in two steps: preparation of the base membrane and coating it. To overcome this, other methods were proposed: delayed demixing and incorporation of surface modifying macromolecules (SMMs).

Delayed demixing is based on shifting the phase boundary line away from the polymer-solvent axis on a polymer (P)-solvent (S)-nonsolvent (N) triangular diagram. This is done by using a nonsolvent (N) with stronger affinity to the polymer. Thus, during the S-N exchange process in the coagulation bath, the P/S/N mixture stays in the enlarged miscible region for a longer period, allowing formation of a thicker skin layer with fewer defects. Yamasaki et al.[2] and Lee et al.[3] used isopropanol, instead of water, as the first nonsolvent in their membrane fabrication by the dry-wet phase inversion method. The membrane was then transferred into water, the second nonsolvent, to complete the phase separation. Using this technique, the skin layer thickness, and consequently the selectivity, increased while the flux decreased with an increase in the period of immersion in isopropanol. Despite a significant improvement in reducing the number of defects, Yamasaki et al.[2] reported that further lamination by silicone rubber was still necessary to stop the leakage.

Correspondence to: D. Rana (rana@eng.uottawa.ca, rana@uottawa.ca) or T. Matsuura (matsuura@eng.uottawa.ca).
Contract grant sponsors: Natural Sciences and Engineering Research Council of Canada.

The second approach is based on preferential migration of a polymer of lower surface energy, called surface modifying macromolecule (SMM), to the surface of the membrane and forming a defect-free surface layer. Macheras et al.[4] proposed a single step process by casting a solution containing two polymers with significantly different surface energies. According to their technique, the membranes can be cast from an appropriate polymer blend solution by dry-wet phase inversion process.

The science behind this technique relies on the thermodynamic incompatibility between the two polymers that causes their demixing. If the mixture is equilibrated in air, the polymer with the lower surface energy (hydrophobic polymer) will concentrate at the air interface to reduce the interfacial tension of the system. The phenomenon has been confirmed by a number of researches.[5–9]

SMMs have been developed aiming at enhancing surface hydrophobicity or hydrophilicity and chemical resistivity of membranes. They are synthesized from a prepolymer containing a soft segment in its structure and end-capped with hydrophobic, hydrophilic or charged functional groups. SMMs could be synthesized with different combinations and stoichiometries of reagents. They have found applications in many processes such as pervaporation, ultrafiltration, and membrane distillation.[10–15]

Suk et al.[10,11] synthesized a SMM starting from a prepolymer with hydrophobic dimethylsiloxane as its soft segment. Together with the fluorohydrocarbon end-capping group, their SMM exhibited high hydrophobicity that facilitated the migration when blended in polyethersulfone solution. The scanning electron microscopy (SEM) image revealed that, in fact, the surface segregation of the SMM layer did occur. Contact angle and X-ray photoelectron spectroscopy (XPS) measurements also confirmed that the SMM was the major component of the surface layer.

In the present work the above two techniques, namely, delayed demixing and SMM incorporation were combined, expecting a synergistic effect to further reduce the number of defects in the skin layer of an asymmetric polysulfone (PSf) membrane. The synthesized SMMs consisted of urea or urethane prepolymer end-capped with compounds with hydrophobic, hydrophilic or charged functional groups. For this purpose, a small amount of SMMs was blended into the solution of the host polymer. The SMM migrated to the surface during casting rendering the surface either hydrophobic, hydrophilic, or charged, depending on the functional group of the added SMM.

EXPERIMENTAL

Materials

Polysulfone (PSf, Udel-3500, pellet) was purchased from the Amoco Performance Products, Atlanta, GA, and was dried in an air circulating oven at 80°C overnight before being used. The weight average molecular weight and polydispersity index were 37 kD and 2.11, respectively. The glass transition temperatures (T_g) at the onset and at the mid point were 184.2 and 187.8°C, respectively. The 4,4′-methylene bis(phenyl isocyanate) (also known as methylene diisocyanate, MDI, 98%); 4-hydroxybenzenesulfonic acid, sodium salt dihydrate (also known as hydroxyl benzene sulfonate, HBS); poly(propylene glycol) (PPG) with typical number average molecular weight 425 Da; and poly(ethylene glycol) (PEG) with typical number average molecular weight 400 Da were obtained from Sigma-Aldrich, St. Louis, MO. The α,ω-aminopropyl poly(dimethyl siloxane) (PDMS) of average molecular weight 900 was obtained from Shin-Etsu Chemical, Tokyo, Japan. Oligomeric fluoro-alcohol (OFA), Zonyl BA-L™ (BAL) of number average molecular weight 443 and 70 wt % fluorine is a DuPont product and was supplied by Aldrich Chemical Company, Milwaukee, WI. The *N*,*N*-dimethylacetamide (DMAc) and isopropyl alcohol (IPA) were purchased from Sigma Aldrich (Canada). DMAc was used as solvent and IPA as nonsolvent of the first coagulation bath. Deionized water (DI) was used as nonsolvent of the second coagulation bath.

SMMs synthesis

The synthesis of surface modifying macromolecules (SMMs) was carried out by two-step condensation polymerization process.[12,13] Three types of SMMs were prepared in this study:

1. Urea prepolymer was initially made by polymerization reaction between MDI and PDMS, and then was end-capped with OFA. This SMM is called nSMM.
2. Urethane prepolymer was initially made by polymerization reaction between MDI and PEG and then was end-capped with HBS. This SMM is called cSMM-PEG.
3. Urethane prepolymer was initially made by polymerization reaction between MDI and PPG and then was end-capped with HBS. This SMM is called cSMM-PPG.

The same molar ratio of the monomers was used in the SMMs synthesis; i.e., MDI:PDMS:OFA = 3 : 2 : 2 for nSMM and MDI:PEG (or PPG):HBS = 3 : 2 : 2 for cSMM-PEG or cSMM-PPG. All reactions were conducted in DMAc solvent. MDI was reacted with PDMS (for nSMM) or PEG or PPG (for cSMM-PEG/-PPG) for 3 h at 48–50°C to synthesize the prepolymers. Then, OFA (for nSMM) or HBS (for cSMM-PEG/-PPG) was added for end-capping which was

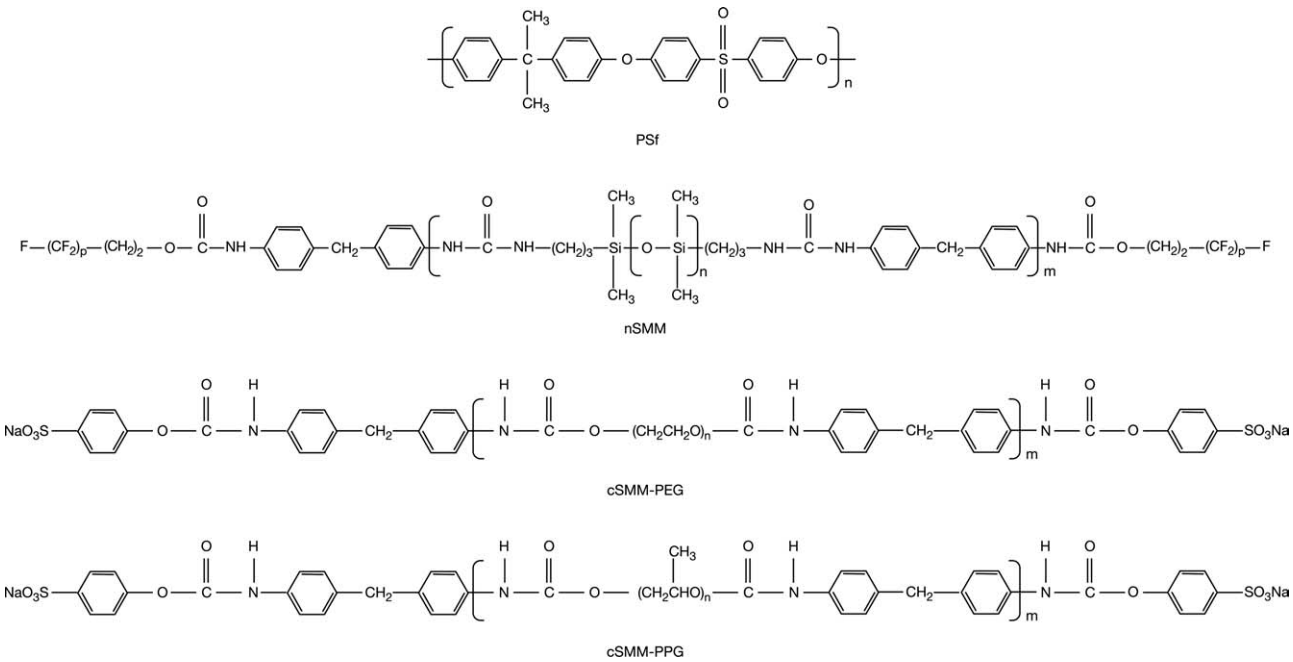

Figure 1 Chemical formula of PSf and SMMs.

carried out for 24 h at the same temperature. After the completion of the reaction, the SMMs were precipitated in water and dried at 50°C. The chemical structures of PSf and SMMs are shown in Figure 1.

SMMs characterization

Glass transition temperature (T_g) was measured by differential scanning calorimeter (DSC Q1000, TA Instruments, New Castle, DE). Around 5 mg of polymer sample was placed into an aluminum pan and was heated to 260°C at a rate of 10°C min^{-1} and maintained there for 10 min. Then, the polymer was cooled to −50°C at the same rate of 10°C min^{-1}. The T_g value was recorded at the onset and mid-point of corresponding heat capacity transition. Other characterization techniques including elemental analysis, molecular weights, polydispersity index, differential scanning calorimetry, and Fourier transform infrared spectroscopy have been previously reported in details.[14,15]

Membrane preparation and characterization

The membranes without SMM were prepared from casting solutions with PSf concentrations of 15, 20, and 25 wt %. For this purpose, the polymer pellet was added to the DMAc solvent and the mixture was gently stirred at 80°C for 12 h in a rotator until the solution became homogeneous.

The casting solutions containing each of the SMMs were prepared following the same method after adding 1.5 wt % of each SMM. A total of 12 types of membranes were produced, the compositions of which are shown in Table I.

TABLE I
Composition of casting solutions

Membrane no.	PSf (wt %)	DMAc (wt %)	nSMM (wt %)	cSMM-PEG (wt %)	cSMM-PPG (wt %)
1	15	85	–	–	–
2	15	83.5	1.5	–	–
3	15	83.5	–	1.5	–
4	15	83.5	–	–	1.5
5	20	80	–	–	–
6	20	78.5	1.5	–	–
7	20	78.5	–	1.5	–
8	20	78.5	–	–	1.5
9	25	75	–	–	–
10	25	73.5	1.5		
11	25	73.5	–	1.5	
12	25	73.5	–	–	1.5

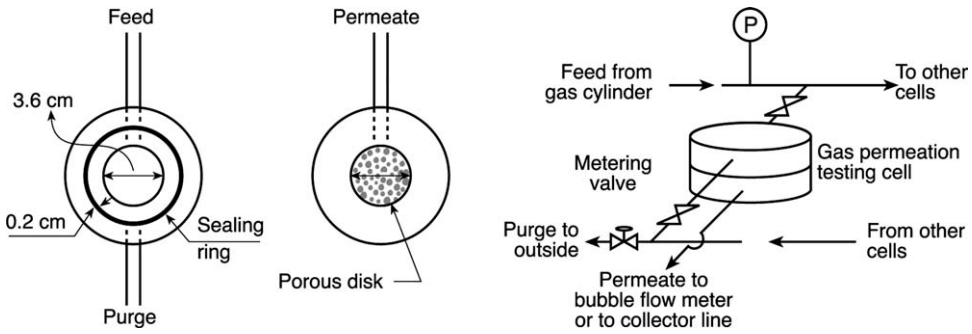

Figure 2 Schematic of gas permeation cell in constant pressure system[16].

The solutions were cast over a glass plate using a casting bar with a 0.25-mm gap. Immediately after casting, the cast film together with the glass plate were immersed into an isopropanol bath (first coagulation bath) for predetermined periods of 10, 30, 60, and 90 s to form the skin layer. Then, the cast film and the glass plate were immersed in a water bath (second coagulation bath) to complete the solvent/nonsolvent exchange process. The membrane was peeled off the glass plate during this stage and was kept in fresh water for one day or more and then vacuum dried at 100°C for 3 days.[3]

Static contact angle measurements

The static contact angle (SCA) measurement of the membrane surface was done using a VCA Optima Surface Analysis System (AST Products, Billerica, MA). The sample was fixed on a slide glass, and then a drop of liquid was placed on the sample surface using a micro syringe (Hamilton Company, Reno, NV). The SCAs were measured at ten different spots on each membrane coupon. The values were averaged and the standard deviation was calculated and recorded.

SEM measurements

A model Tescan Vega-II XMU variable pressure SEM (VPSEM), Tescan USA, Cranberry Twp., PA, was used to generate the SEM photographs. Membrane samples were fractured cryogenically by immersing in liquid nitrogen and were mounted in chair-shaped sample holders with double-sided tape. Fractured surfaces were sputter coated under vacuum with a thin layer of 60% gold and 40% palladium in a sputter system (Hummer VII, Anatech, Springfield, VA).

XPS measurements

The elemental composition at the surface of each membrane sample was determined by X-ray photoelectron spectroscopy (XPS, Kratos Axis HS X-ray photoelectron spectrometer, Manchester, UK). Samples of 1 cm^2 area were cut randomly from the membrane. Monochromatized Al Kα X-radiation was used for excitation. A 180° hemispherical analyzer with a three channel detector was employed. The X-ray gun was operated at 15 kV and 20 mA. The pressure in the analyzer chamber was 1.33×10^{-4} to 1.33×10^{-5} Pa. The size of the analyzed area was about 1 mm^2. All the membrane samples were analyzed for specific element content at both top and bottom surfaces.

Gas permeation measurements

Gas permeation tests were performed using pure nitrogen (N_2) and pure oxygen (O_2) as test gases using a constant pressure (CP) system consisting of three parallel cells. The schematic of the gas permeation cell is shown in Figure 2. A circular membrane sample with an effective permeation area of 10.2 cm^2 was placed at the bottom of the cell over a paper filter on top of a porous metal disk. The seal was made by a 2-mm wide and 0.2-mm high semi-circular metal ring on the upstream and a flat metal surface on the downstream parts of the cell. To prevent a potential damage to the membrane by the edge of the sealing ring, the feed (upstream) side of the membrane was laminated with a paraffin film ring. Feed pressure was set at 105 psig (~ 120 psia) while the permeate side was maintained at atmospheric pressure. Experiments were carried out at ambient temperature. The gas permeation rate was measured by a soap bubble flow meter. Each experiment was carried out in triplicate to ensure reproducibility and the average of the results was reported.

Theory

The permeance (P/l) defined as pressure-normalized flux, is calculated by:

$$\left(\frac{P}{l}\right) = \frac{Q_p}{A\Delta p} \times 10^6 = \frac{F}{\Delta p} \times 10^6 \qquad (1)$$

where (P/l) is the permeance, GPU (gas permeation unit = 10^{-6} cm^3 (STP)/cm^2 s cmHg), Q_p is the

TABLE II
Structural Details of the SMMs and their Solubility Parameters

SMM	*n*	*m*	*P*	Solubility parameter [(cal cm^{-3})$^{1/2}$]
nSMM	9.81	10.14	7.58	9.32
cSMM-PEG	8.68	6.17	–	11.45
cSMM-PPG	7.02	8.99	–	10.74

m, *n*, and *p* are the number of repeating units in the polymer structure as specified in Figure 1.

permeation rate, cm^3(STP)/s, A is the permeation area of the membrane, cm^2, Δp is the pressure difference across the membrane, cmHg, and F is the permeation flux, cm^3 (STP)/cm^2 s.

The ideal selectivity of gas A over gas B (α°_{AB}) is calculated as follows:

$$\alpha^{\circ}_{AB} = \frac{(P/l)_A}{(P/l)_B} \quad (2)$$

The permeance and the ideal selectivity were calculated using eqs. (1) and (2). Each experiment was triplicated to ensure reproducibility.

RESULTS AND DISSCUSSION

SMMs characterization

Glass transition temperatures (T_gs) of cSMM-PEG at the onset and the mid point were 6.8 and 13.4°C, respectively. The T_gs of cSMM-PPG at the onset and the mid point were −18.3 and −11.6°C, respectively. The T_gs of the nSMM were >280°C. The precise T_g values of the latter could not be obtained due to the equipment limitation.

The structural parameters of the SMMs were previously determined and reported.[14,15] The *n*, *m*, and *P* values, referring to the repeating units in the polymer structure as specified in Figure 1, for nSMM, cSMM-PEG, and cSMM-PPG are summarized in Table II.[14,15] The solubility parameters of the SMMs were calculated by applying the additivity rule for the structural components of each SMM.[17,18] The detailed calculations are described in the appendix.

SCA characteristics

The SCA results are summarized in Table III. The results indicated that the SCA of the membranes increased by adding nSMM and decreased by adding cSMMs. In other words, addition of nSMM made the surface of the PSf membrane more hydrophobic while cSMMs made the membrane more hydrophilic. This observation suggests that SMMs impose their intrinsic characteristics to the membrane by migrating to the surface during either casting or coagulation process.

SEM analysis

Figure 3 shows the SEM images of the cross-sections of three PSf membranes. These membranes were prepared from 25 wt % polymer solution without the addition of SMMs, immersed in isopropanol for 30, 60, and 90 s, respectively. As shown, the thickness of the skin layer in the membrane with 30-s immersion time is ~ 5 μm, while that in the membrane with 90-s immersion time increased to >10 μm.

Figure 4 shows the cross-section of a PSf–nSMM membrane with large defective pores at the membrane surface and irregular macro-voids underneath.

Figure 5 shows the SEM images of the cross-sections of three PSf-cSMM-PPG membranes. These membranes were prepared from 25 wt % PSf and 1.5 wt % cSMM-PPG, with 30, 60, and 90 s of isopropanol immersion time. As seen in the figures, a dense skin layer thicker than 10 μm was formed even at 30-s immersion time. Furthermore, the support layer changed from large irregular macro-voids (as seen in case of nSMM, Fig. 4) to sponge-like pores. The reason could be due to the decrease in the solvent/nonsolvent exchange rate.

In summary, the SEM photographs suggested that a thick and defect-free skin layer could be formed by increasing the immersion time of the membrane in isopropanol and/or by the addition of hydrophilic SMMs such as cSMM-PPG.

XPS analysis

Table IV reports the theoretical mass concentrations of the select elements—including sulfur (S), oxygen (O), nitrogen (N), silicone (Si), and sodium (Na)—in PSf, nSMM, and cSMM-PPG polymers. Table V tabulates the theoretical mass concentrations of the select elements in the base PSf membrane as well as in two of the SMM-incorporated membranes assuming that the SMMs were uniformly dispersed in the base membrane. Finally, Table VI shows the XPS-measured mass concentrations of the select elements at the top and the bottom surfaces of three of the

TABLE III
SCA Data of PSf and PSf Containing SMM Membranes

Membrane type	SCA (°)
PSf	76.4 ± 2.3
PSf containing nSMM	105.8 ± 2.5
PSf containing cSMM-PEG	66.3 ± 2.4
PSf containing cSMM-PPG	69.5 ± 3.6

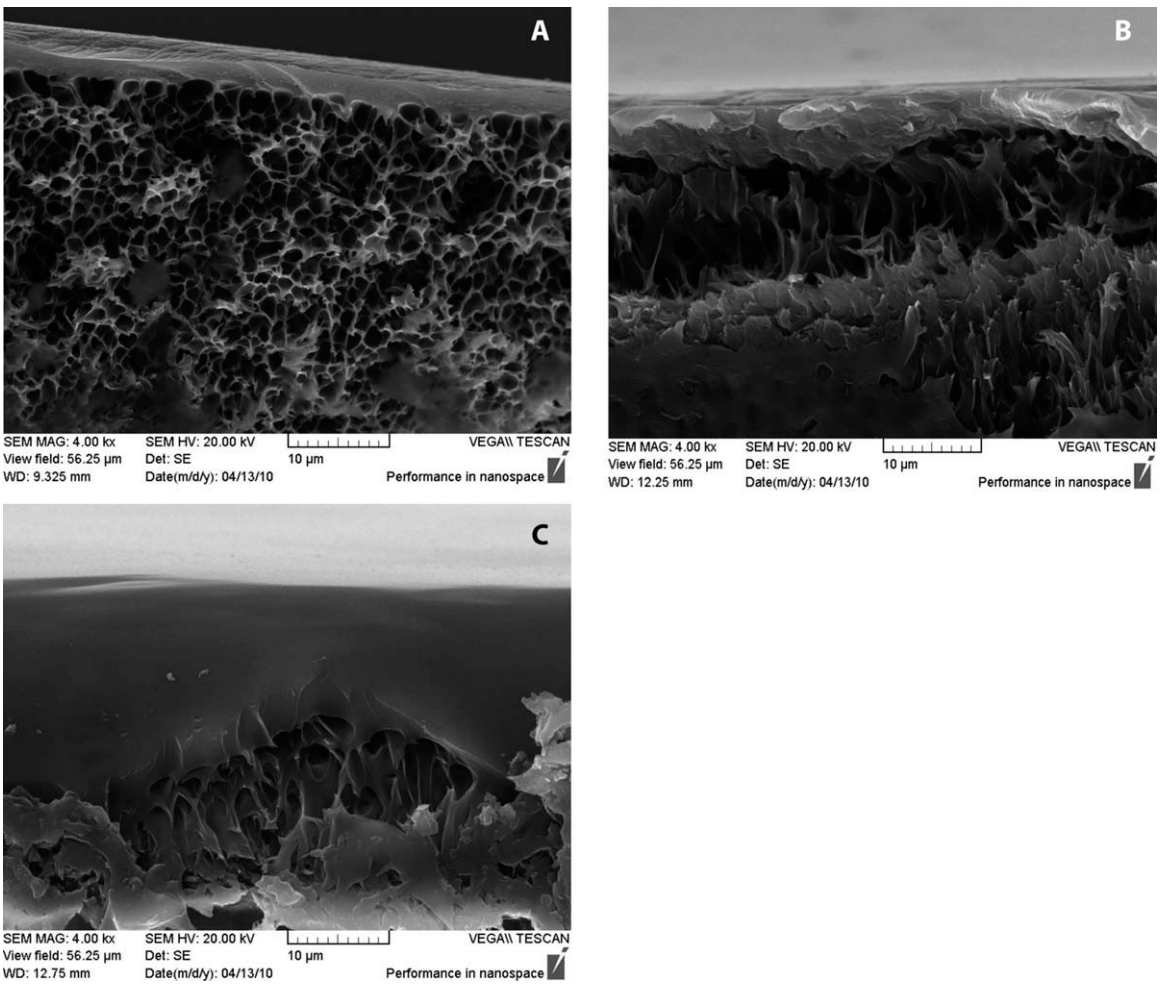

Figure 3 Cross-sectional SEM images of three PSf membranes without the addition of SMMs. A: PSf concentration: 25 wt%; immersion time in isopropanol: 30 s. B: PSf concentration: 25 wt%; immersion time in isopropanol: 60 s. C: PSf concentration: 25 wt%; immersion time in isopropanol: 90 s.

experimental membranes at the shortest (10 s) and the longest (90 s) immersion times. Interpretation of the results according to the individual elemental mass concentrations follows.

Si and Na

Because silicone exists only in nSMM and sodium only in cSMM-PPG, these two elements act as atomic markers for the two respective SMMs. If SMMs are uniformly distributed across the cross-section of the membrane, the mass concentrations of Si and Na in the PSf-nSMM and PSf-cSMM-PPG membrane would be the same as the values shown in Table V. The experimental values in Table VI are significantly greater than the calculated values (Table V). Hence it can be concluded that SMMs migrated toward the membrane surfaces. Furthermore, the mass concentrations at the top surface are higher than the bottom surface, indicating faster SMM migration to the top surface than the bottom surface.

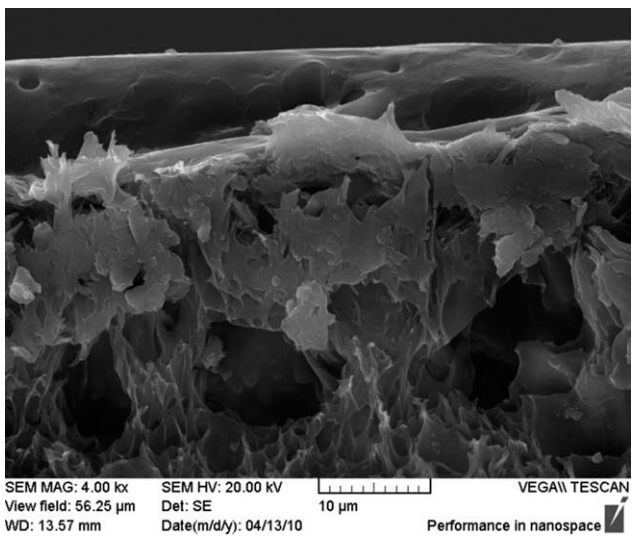

Figure 4 Cross-sectional SEM image of PSf-nSMM membrane. PSf concentration: 25 wt%; immersion time in isopropanol: 90 s.

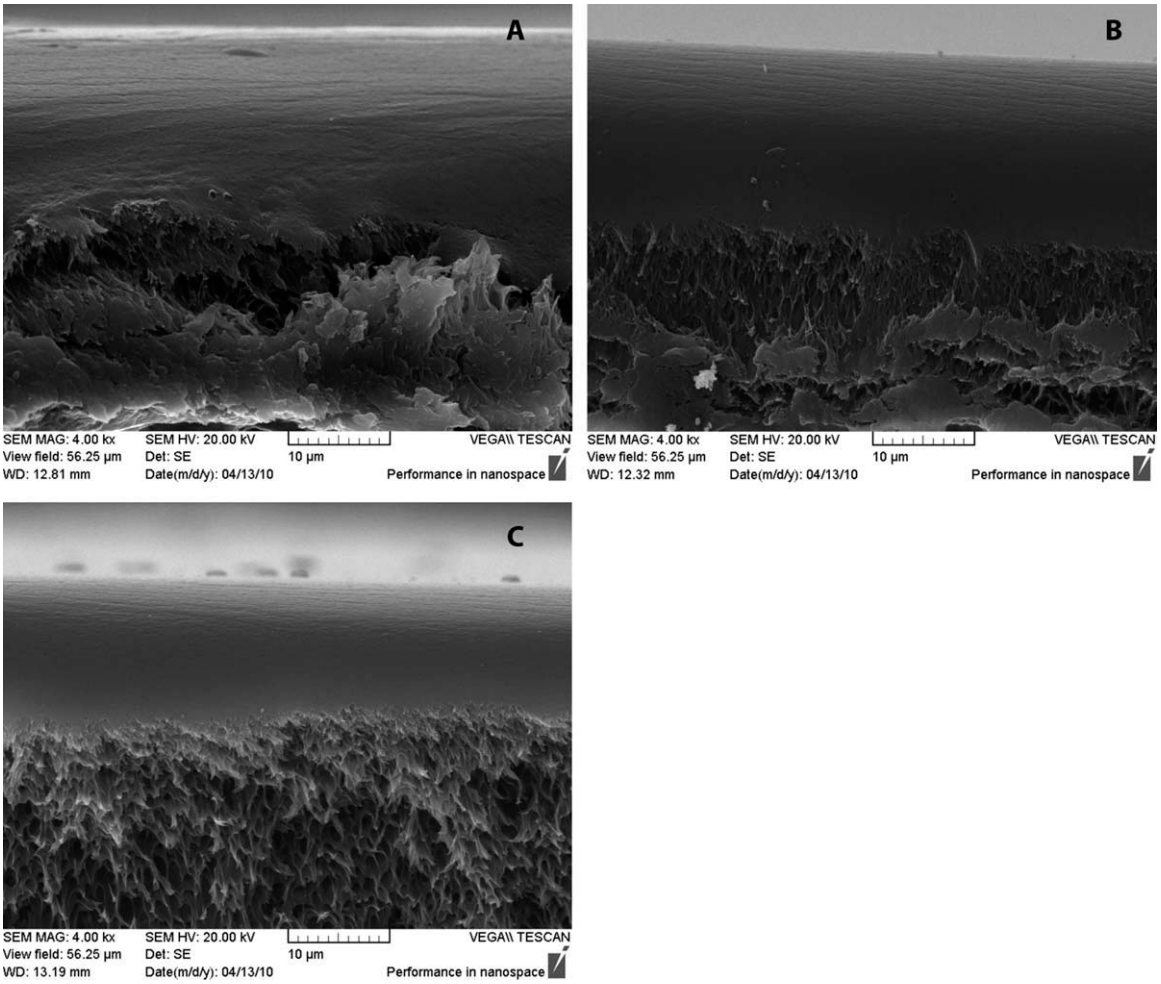

Figure 5 Cross-sectional SEM images of three PSf-cSMM-PPG membranes. A: PSf concentration: 25 wt%; immersion time in isopropanol: 30 s. B: PSf concentration, 25 wt%; immersion time in isopropanol, 60 s. C: PSf concentration: 25 wt%; immersion time in isopropanol: 90 s.

S and N

Sulfur exists in PSf and to a small extent in the two cSMMs. Nitrogen exists only in the SMMs, but not in PSf. Therefore, it is expected that after mixing PSf and any of the SMMs, sulfur becomes diluted and nitrogen is concentrated. Furthermore, if more SMMs migrate to the top surface than the bottom surface, less sulfur and more nitrogen will be detected at the top surface. The XPS measurements of all the samples confirmed these expectations.

TABLE IV
Theoretical Mass Concentration of Select Elements in PSf and SMMs

	Mass concentrations (%)				
Polymers	S	O	N	Si	Na
PSf	7.2	14.5	–	–	–
nSMM	–	15.5	4.7	23.8	–
cSMM-PPG	0.1	23.9	4.2	–	0.68

O

Oxygen is not an atomic marker for any of the macromolecular components. However, closeness of the experimental values (Table VI) to the theoretical ones (Tables IV and V) can be used as a measure of accuracy of the XPS measurements.

TABLE V
Theoretical Mass Concentration of Select Elements in the Membrane Assuming SMMs Were Uniformly Dispersed in PSf[a]

	Mass concentrations (%)				
Membranes	S	O	N	Si	Na
PSf	7.2	14.5	–	–	–
PSf-nSMM	6.5	14.6	0.43	2.1	–
PSf-cSMM-PPG	6.6	15.3	0.38	–	0.06

[a] PSf and SMM concentrations in the casting dope are 15 and 1.5 wt %, respectively.

TABLE VI
Mass Concentration of Select Atoms Measured by XPS at the Top and Bottom Surfaces of the Prepared Membranes

Membrane		Mass concentrations (%)				
Base polymer-SMM-immersion time		S	O	N	Si	Na
PSf-10	Top	4.08	15.52	–	–	–
	Bottom	5.76	14.23	–	–	–
PSf-90	Top	2.47	13.67	–	–	–
	Bottom	3.01	22.72	–	–	–
PSf-nSMM-10	Top	2.17	20.04	4.13	14.19	–
	Bottom	1.53	14.46	3.63	10.13	–
PSf-nSMM-90	Top	2.94	21.00	4.26	14.47	–
	Bottom	1.15	15.83	4.10	10.17	–
PSf-cSMM(PPG)-10	Top	0.54	20.33	4.91	–	0.61
	Bottom	3.29	18.20	2.86	–	0.41
PSf-cSMM(PPG)-90	Top	1.65	18.14	3.22	–	0.86
	Bottom	3.13	17.90	2.80	–	0.68

PSf and SMM concentrations in the casting dope are 15 and 1.5 wt %, respectively.

In summary, the XPS results suggest that SMMs migrated to the top surfaces of the membrane samples under all experimental conditions.

Gas permeation results

Effects of immersion time

Figure 6(a,b) show the oxygen permeance and oxygen/nitrogen ideal selectivity of the base PSf membranes with no SMMs. The membranes were prepared using three different polymer concentrations of 15, 20, and 25 wt %, and were immersed in isopropanol non-solvent for four different time periods of 10, 20, 60, and 90 s.

From the figures, it can be seen that oxygen permeance decreased and oxygen/nitrogen ideal selectivity increased with an increase in the immersion time. The results confirmed the observations from the SEM images as shown in Figure 3(a,b), where a thicker skin layer formed at immersion time of 90 s was expected to enhance the selectivity and reduce the permeability of the membrane. The results are also in agreement with those reported by Yamasaki et al.[2] and Lee et al.[3] However, the permeances obtained in the present work were lower than those reported by Lee et al.[3] This could be due to the formation of tighter pores underneath the skin layer imposing a greater resistance to the gas flow, or to random performance of membrane coupons.

Also, a tendency was observed in oxygen permeance to decrease, and the selectivity to increase with an increase in PSf concentration. The general trend suggests that the polymer concentration imposed a similar effect as the immersion time.

Effects of SMMs

Figure 7(a,b) show the performance of the PSf membranes including hydrophobic nSMM. The PSf concentrations and the isopropanol immersion times were the same as in the previous experiments.

Compared to the results from the base PSf membranes, as shown in Figure 6(a,b), the nSMM

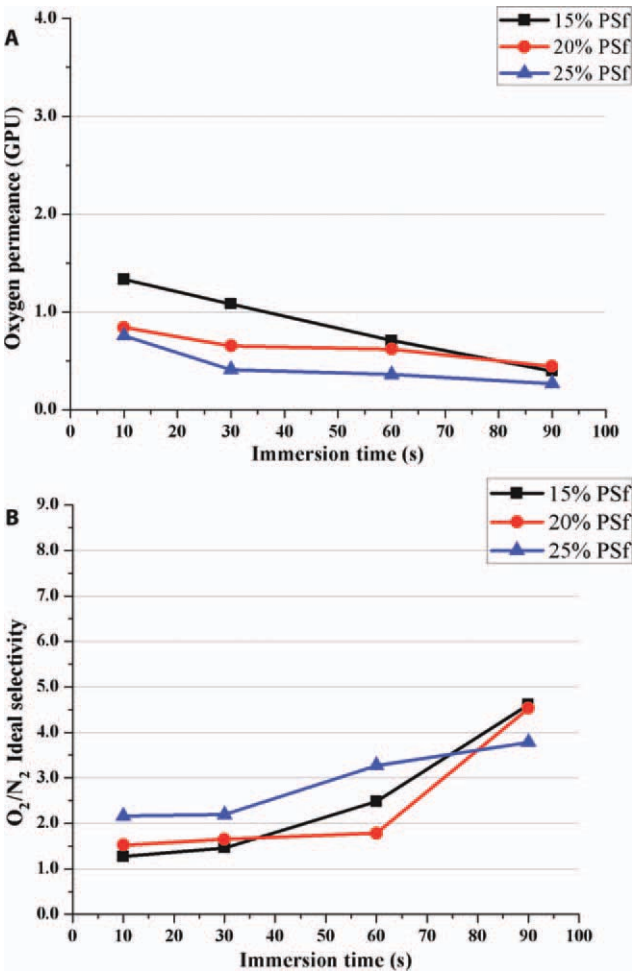

Figure 6 Oxygen permeance (a) and O_2/N_2 ideal selectivity, (b) of the PSf membranes at different immersion times. [Color figure can be viewed in the online issue, which is available at wileyonlinelibrary.com.]

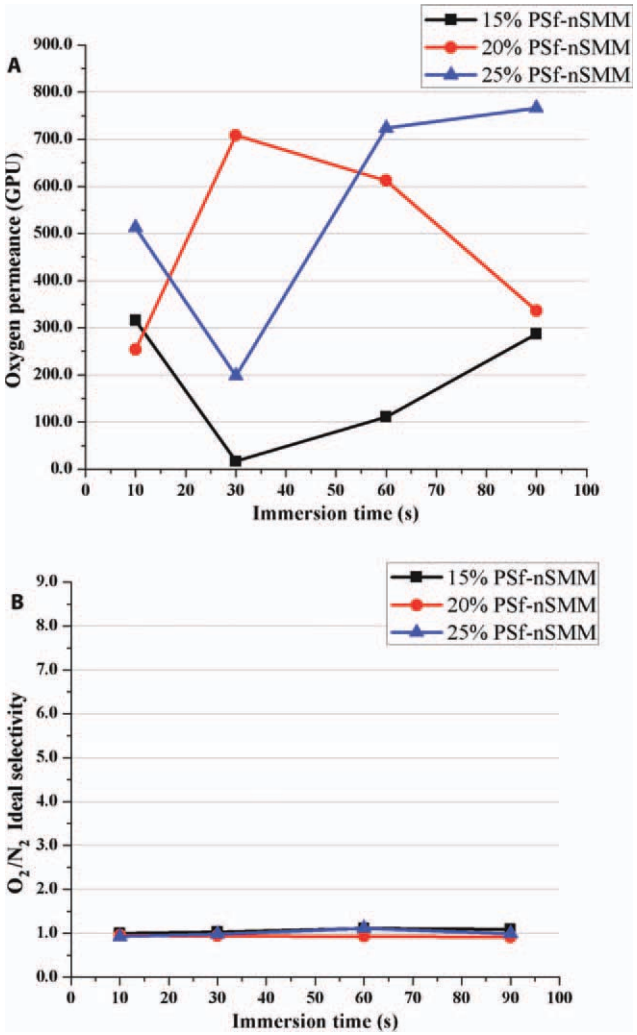

Figure 7 Oxygen permeance (a) and O_2/N_2 ideal selectivity, (b) of the membranes with nSMM blending. [Color figure can be viewed in the online issue, which is available at wileyonlinelibrary.com.]

incorporated membranes exhibited permeances that were orders of magnitude higher [Fig. 7(a)], while the ideal selectivities were nearly equal to unity [Fig. 7(b)]. The effects of PSf concentration and isopropanol immersion time were random. The results indicated that addition of nSMM promoted formation of large and defective pores. This observation is in agreement with those from the SEM image shown in Figure 4.

Figure 8(a,b) show the performance of PSf membranes incorporating charged cSMM-PPG. The immersion times and PSf concentrations were the same as in the previous experiments.

In general, the trends observed in this set of experiments were similar to those with PSf membranes without SMM incorporation, as shown in Figure 6(a,b). That is, the permeance decreased and ideal selectivity increased with increasing either immersion time or polymer concentration. Major improvements were observed in both permeance and ideal selectivity of the membranes. The permeances of the membranes with 15 and 20 wt % of PSf increased by an average of 60%. On the other hand, the permeance of the membrane with 25 wt % PSf showed slight decrease compared with similar membrane without SMM.

The ideal selectivities also increased significantly and reached a maximum value of 8 for 25 wt % PSf-cSMM-PPG sample at the immersion time of 60 s. The same membrane also showed ideal selectivities of above seven for immersion times of 30 and 90 s. The membrane prepared from 15 and 20 wt % PSf also exhibited higher ideal selectivities compared to the base membrane [Fig. 6(b)]. The results were in agreement with the observations from the SEM images shown in Figure 5. They also support the hypothesis of migration of SMMs to the top surface of

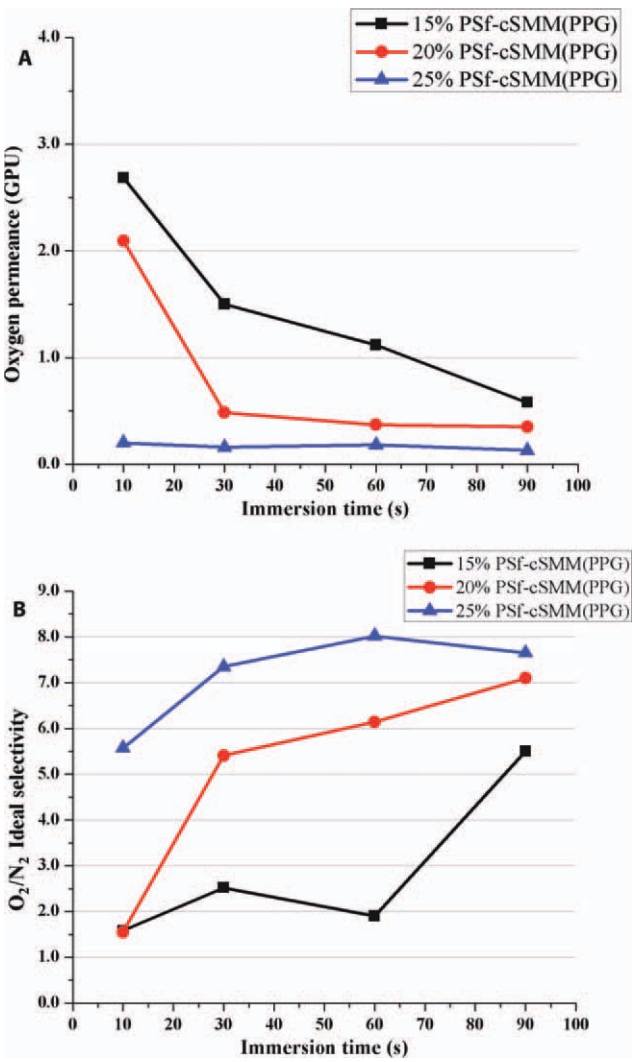

Figure 8 Oxygen permeance (a) and O_2/N_2 ideal selectivity, (b) of the PSf-cSMM-PPG membrane. [Color figure can be viewed in the online issue, which is available at wileyonlinelibrary.com.]

the membrane as was also supported by the XPS results.

Figure 9(a,b) show the performance of the PSf membranes including charged cSMM-PEG. The immersion times and PSf concentrations were the same as in the previous experiments.

Comparing Figures 8(a) and 9(a), the permeances and their variations of the PSf-cSMM-PEG membranes were smaller than those of the PSf-cSMM-PPG membranes. The permeances were nearly independent of immersion time and polymer concentration. As a result, the ideal selectivity values, as shown in Figure 9(b), were also nearly independent of immersion time and polymer concentration. The latter values were between 4 and 5. This observation signifies the fact that a thick skin layer was developed almost immediately after immersion of the cast film in isopropanol. From a different perspective, a comparison between the PSf-cSMM-PEG membranes and the base PSf membranes reveal that the selectivity of the membranes improved by the addition of the cSMM-PEG.

Summary of gas permeation results

- Incorporation of SMMs has definite effects on the performance of PSf membranes in permeation of oxygen and nitrogen under all experimental conditions.
- nSMM negatively affects the performance of the membrane by rendering it non-selective toward oxygen and nitrogen.
- cSMM-PPG and cSMM-PEG improve the ideal selectivity of the membrane. The former offers the highest ideal selectivity among the experimental membranes.
- The permeance and ideal selectivity are affected by isopropanol immersion time as well as polymer concentration. The trend is that permeance decreases and ideal selectivity increases with an increase either in immersion time or polymer concentration. The best results were achieved when the cast membrane was kept in isopropanol for more than 30 s.

Discussions based on phase diagram

The results discussed so far including SCA, SEM, XPS, and gas permeation experiments suggested that the SMMs migrated to the surface of the membrane and modified the membrane properties. This section is aimed at explaining the experimental results by shift of phase boundary lines in the P—S—N triangular diagram at the SMM dominant surface layer.

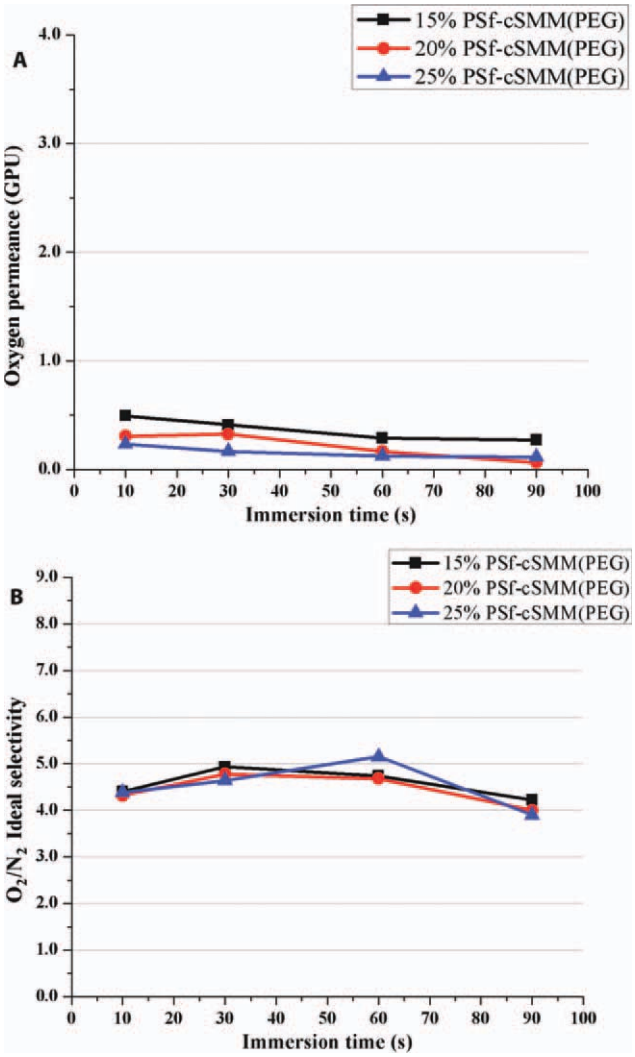

Figure 9 Oxygen permeance (a) and O_2/N_2 ideal selectivity, (b) of the PSf-cSMM-PEG membrane. [Color figure can be viewed in the online issue, which is available at wileyonlinelibrary.com.]

It is well understood that the interaction between an organic liquid and a polymer becomes stronger when the difference between their solubility parameters becomes smaller.[17] It is also known that the Flory–Huggins interaction constant becomes smaller as the interaction becomes stronger. Considering the interaction between nonsolvent (N) and polymer (P) on the polymer (P)-solvent (S)-nonsolvent (N) triangular diagram, the lower N/P interaction parameter shifts the phase boundary line away from the P-S axis, as shown in Figure 10. That is, because of the stronger N/P affinity, polymer can tolerate a larger amount of N in the P/S/N mixture. Thus, the miscibility gap is broadened, which increases the time for the composition path to reach the phase boundary line during the S-N exchange process. This enhances the possibility of delayed demixing during the coagulation process, allowing for the dense skin layer to

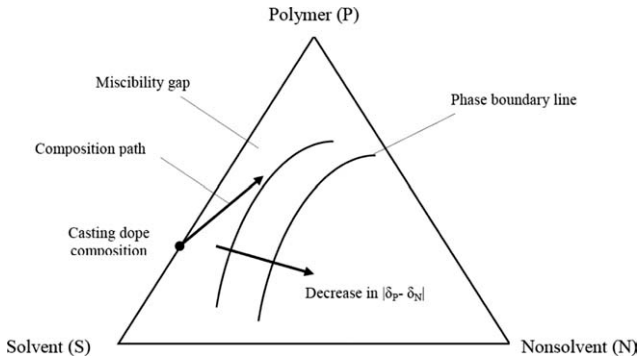

Figure 10 Effect of solubility parameter change on the phase boundary line and the miscibility gap.

grow before the phase boundary line is crossed. This results in the formation of a thicker and more selective layer with smaller number of defects. The cause and effect relationship described above is schematically illustrated in Scheme 1 and Figure 10.

To discuss the effects of varying solubility parameter when either N or P is changed, it is assumed that solubility parameter of P can be represented by that of SMM when present. This assumption is valid because it has been shown earlier that SMMs migrate to the surface of the membrane accumulating at the N–P interface. The solubility parameter of isopropanol and PSf were calculated by applying the additivity rule for the structural components of isopropanol molecule and the structural components of the repeat unit of PSf.

1. Changing the nonsolvent from water to isopropanol
   The relative positions of the solubility parameter of P (PSf) and the two Ns (water and isopropanol) are shown below together with the numerical values of their solubility parameters ($(\text{cal cm}^{-3})^{1/2}$).

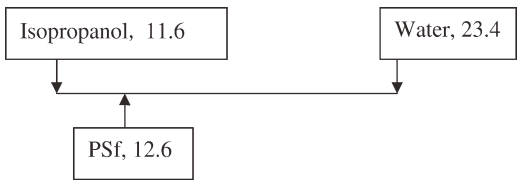

   Solubility parameter of PSf is much closer to isopropanol than to water. This suggests that replacing water with isopropanol as non-solvent would result in the formation of a thicker skin layer (lower permeance) and smaller number of defective pores (higher selectivity). This explains the results shown in Figure 6.
2. Change in the polymer at the N/P interface from PSf to nSMM

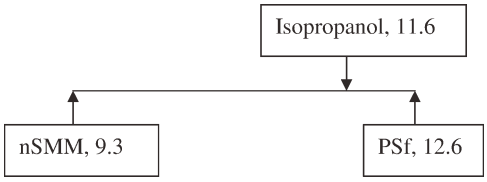

   As shown in the schematic above, the solubility parameter of isopropanol is closer to that of PSf than to nSMM. This suggests that the delayed demixing has a greater chance with PSf/isopropanol system than with nSMM/isopropanol. Therefore, the latter system encourages a rapid crossing of the phase boundary line, resulting in the formation of defective pores. This corresponds to the results shown in Figure 7.
3. Changing the polymer at the cast film surface from PSf to cSMM-PPG or -PEG

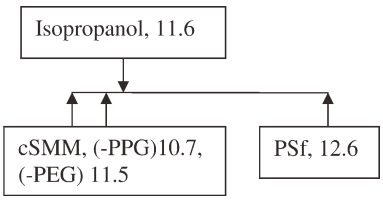

When the surface of the membrane is enriched with cSMMs the solubility parameters of P/N are the most compatible of all the experimental scenarios. The differences in solubility parameters between both cSMMs (P) and isopropanol (N) are much less than that between PSf (P) and isopropanol. They increase the chance of delayed demixing considerably. As a result, the composition path stays in the miscibility gap for a longer period, making the dense layer thicker and less imperfect. This trend is seen most clearly in Figure 8 particularly for the membranes made from the casting dopes with 20 and 25 wt % PSf.

Fine tuning of cSMM was possible by changing the prepolymer structure. For example, by changing

Smaller difference in P/N solubility parameter
↓
Lower Flory-Huggins constant
↓
Broadening of miscibility gap
↓
Delayed demixing
↓
Formation of thicker and less imperfect skin layer

Scheme 1 Effect of solubility parameter on the dense layer formation.

the soft segment of the prepolymer PPG to PEG, the solubility parameter increases. This is because the SMM-PEG is more hydrophilic than SMM-PPG. This small change in solubility parameter did not necessarily predict the observed trend (from Figs. 8 to 9) in the membrane performance. The reason is that the membrane surface would not be perfectly covered by the SMM and therefore, would not meet the theoretical expectations.

CONCLUSIONS

1. An integrally asymmetric membrane with fewer defective pores can be fabricated by immersing the cast polymer film into isopropanol instead of water, which demonstrates stronger affinity to the polymer.
2. Thicker and less imperfect skin layer was formed at longer immersion times within the experimental range of 10–90 s. This resulted in lower permeance and higher ideal selectivity for oxygen and nitrogen.
3. SMMs migrate to the surface of the membrane when mixed with the polymer solution.
3. Among the three SMMs tested in this study, nSMM negatively affected the membrane's performance by rendering it non-selective. The phenomenon was explained by encouraging the formation of large and defective pores in the selective skin layer of the membrane.
4. The other two SMMs including cSMM-PPG and cSMM-PEG improved the selectivity of the PSf membrane by enhancing the thickness of the skin selective layer and preventing formation of defective pores.

The authors are grateful to Dr. C. Feng for the invaluable suggestions during the course of the study, and Mr. L. Trembley, Mr. F. Ziroldo, and Mr. G. Nina of the machine shop of the Department of Chemical and Biological Engineering of the University of Ottawa for their kind assistance in setting up the experimental apparatus.

APPENDIX: CALCULATION OF SOLUBILITY PARAMETERS

The solubility parameter can be calculated by applying additivity rules to the structural components of the repeat unit of the macromolecule and to those of the solvent molecule, by the following equation[17,18]:

$$\delta_{sp} = \sqrt{\frac{\sum E_{coh}}{\sum V}} \quad (1)$$

where δ_{sp} is solubility parameter, $(\text{cal cm}^{-3})^{1/2}$, E_{coh} is heat of vaporization, cal mol^{-1}, V is molar volume, $\text{cm}^3\ \text{mol}^{-1}$.

Physico-Chemical Values of Solubility Parameter for cSMM-PEG

Structural Component	OH	SO_2	$-C_6H_4-$	$-NHCOO-$	$-CH_2-$	$-O-$
No. of repeating units	2	2	$4 + 2 \times 6.17$	$2 + 6.17$	$1 + 2 \times 8.68 \times 6.17 + 6.17$	$(8.68 - 1) \times 6.17$
E_{coh_i} (cal mol^{-1})	7120	9350	7630	6300	1180	800
V_i ($\text{cm}^3\ \text{mol}^{-1}$)	10	23.6	52.4	18.5	16.1	3.8

$$\sum E_{coh_i} = (2)(7120) + (2)(9350) + (4 + 2^*6.17)(7630) + (2 + 2^*6.17)(6300) + (1 + 2^*8.68^*6.17 + 6.17)(1180) + (8.68 - 1)^*6.17(800) = 420716.496(\text{cal/mol})$$

$$\sum V_i = (2)(10) + (2)(23.6) + (4 + 2^*6.17)(52.4) + (2 + 2^*6.17)(18.5) + (1 + 2^*8.68^*6.17 + 6.17)(16.1) + \{(8.68 - 1)^*6.17\}(38) = 3208.69(\text{cm}^3/\text{mol})$$

$$\delta_{sp} = \sqrt{\sum E_{coh} \Big/ V} = \sqrt{\frac{420716.496}{3208.69}} = 11.45(\text{cal/cm}^3)^{1/2}$$

Physico-Chemical Values of Solubility Parameter for cSMM-PPG

Structural component	OH	SO_2	$-C_6H_4-$	$-NHCOO-$	$-CH_2-$	$-O-$	$-CH_3$	$>CH-$
No. of repeating units	2	2	$4 + 2 \times 8.99$	$2 + 2 \times 8.99$	$1 + 1 \times 7.02 \times 8.99 + 8.99$	$(7.02 - 1) \times 8.99$	$1 \times 7.02 \times 8.99$	$1 \times 7.02 \times 8.99$
E_{coh_i} (cal mol^{-1})	7120	9350	7630	6300	1180	800	1125	820
V_i ($\text{cm}^3\ \text{mol}^{-1}$)	10	23.6	52.4	18.5	16.1	3.8	33.5	−1

$\delta_{sp} = 10.74\ (\text{cal cm}^{-3})^{1/2}$

Physico-Chemical Values of Solubility Parameter for nSMM

Structural component	—F	—CF_2—	—CH_2—	—NHCOO—	—C_6H_4—	—NHCONH—	—CH_3	Si	—O—
No. of repeating units	2	2 × 7.58	5 + 6 × 10.14	2	2 + 2 × 10.14	2 × 10.14	(2 + 2 × 9.81) × 10.14	(1 + 9.81) × 10.14	9.81 × 10.14
E_{coh_i} (cal mol^{-1})	1000	1020	1180	6300	7630	12000	1125	810	800
V_i (cm^3 mol^{-1})	18	23	16.1	18.5	52.4	20	33.5	0	3.8

$\delta_{sp} = 9.32$ (cal $cm^{-3})^{1/2}$

Based on aforementioned equation the numerical values assigned to each structural component of each SMM are summarized below. It should be mentioned that the solubility parameters of solvent and PSf used were obtained from above-mentioned reference.

References

1. Henis, J. M. S.; Tripodi, M. K. J Membr Sci 1981, 8, 233.
2. Yamasaki, A.; Tyagi, R. K.; Fouda, A. E.; Matsuura, T.; Jonasson, K. J Membr Sci 1997, 123, 89.
3. Lee, W. J.; Kim, D. S.; Kim, J. H. Korean J Chem Eng 2000, 17, 143.
4. Macheras, J. T.; Bikson, B.; Nelson, J. K. US Patent 5,910,274, 1999.
5. Ward, R. S.; White, K. A.; Hu, C. B. In Polyurethanes in Biomedical Engineering; Planck, H., Egbers, G., Syre I., Eds.; Elsevier: Amsterdam, 1984.
6. Pan, D. H.-K.; Prest, W. M., Jr. J Appl Phys 1985, 58, 2861.
7. Bhatia, Q. S.; Pan, D. H.; Koberstein, J. T. Macromolecules 1988, 21, 2166.
8. Thomas, H. R.; O'Malley, J. J. Macromolecules 1979, 12, 323.
9. Schmidt, J. J.; Gardella, J. A., Jr.; Salvati, L., Jr. Macromolecules 1989, 22, 4489.
10. Suk, D. E.; Matsuura, T.; Park, H. B.; Lee, Y. M. J Membr Sci 2006, 277, 177.
11. Suk, D. E. Development of surface modifying macromolecule blended polyethersulfone membranes for vacuum membrane distillation. Ph.D. Thesis, University of Ottawa, 2006.
12. Rana, D.; Matsuura, T.; Narbaitz, R. M.; Feng, C. J Membr Sci 2005, 249, 103.
13. Rana, D.; Matsuura, T.; Narbaitz, R. M. J Membr Sci 2006, 282, 205.
14. Mohd Norddin, M. N. A.; Ismail, A. F.; Rana, D.; Matsuura, T.; Tabe, S. J Membr Sci 2009, 328, 148.
15. Qtaishat, M.; Rana, D.; Khayet, M.; Matsuura, T. AIChE J 2009, 55, 3145.
16. Kruczek, B. Development and characterization of dense membranes for gas separation made from high molecular weight sulfonated poly(phenylene oxide): Effect of casting conditions on the morphology and performance of the membranes. Ph.D. Thesis, University of Ottawa, 1998.
17. Mulder, M. Basic Principles of Membrane Technology, 2nd ed.; Kluwer Academic Publishers: Dordrecht, 1996.
18. Matsuura, T. Synthetic Membranes and Membrane Separation Processes, 2nd ed.; CRC Press: Boca Raton, FL, 1994.